Structural evolution study of additions of Sb_2S_3 and CdS into GeS_2 chalcogenide glass by Raman spectroscopy*

Hai-Tao Guo(郭海涛)[1,2,†], Ming-Jie Zhang(张鸣杰)[1,3], Yan-Tao Xu(许彦涛)[2], Xu-Sheng Xiao(肖旭升)[2], and Zhi-Yong Yang(杨志勇)[1,‡]

[1] *Jiangsu Key Laboratory of Advanced Laser Materials and Devices, School of Physics and Electronic Engineering, Jiangsu Normal University, Xuzhou* 221116, *China*

[2] *State Key Laboratory of Transient Optics and Photonics, Xi'an Institute of Optics and Precision Mechanics, Chinese Academy of Sciences (CAS), Xi'an* 710119, *China*

[3] *State Key Laboratory of Silicate Materials for Architectures, Wuhan University of Technology, Wuhan* 430070, *China*

(Received 29 April 2017; revised manuscript received 1 June 2017; published online 10 September 2017)

The structures of pseudo-binary GeS_2–Sb_2S_3, GeS_2–CdS, Sb_2S_3–CdS, and pseudo-ternary GeS_2–Sb_2S_3–CdS chalcogenide systems are systematically investigated by Raman spectroscopy. It is shown that a small number of [S_3Ge–GeS_3] structural units (SUs) and -S-S-/S_8 groups exist simultaneously in GeS_2 glass which has a three-dimensional continuous network backbone consisting of cross-linked corner-sharing and edge-sharing [GeS_4] tetrahedra. When Sb_2S_3 is added into GeS_2 glass, the network backbone becomes interconnected [GeS_4] tetrahedra and [SbS_3] pyramids. Moreover, Ge atoms in [S_3Ge–GeS_3] SUs tend to capture S atoms from Sb_2S_3, leading to the formation of [S_2Sb–SbS_2] SUs. When CdS is added into GeS_2 glass, [Cd_4GeS_6] polyhedra are formed, resulting in a strong crystallization tendency. In addition, Ge atoms in [S_3Ge–GeS_3] SUs tend to capture S atoms from CdS, resulting in the dissolution of Ge–Ge bond. Co-melting of Sb_2S_3 or CdS with GeS_2 reduces the viscosity of the melt and improves the homogeneity of the glass. The GeS_2 glass can only dissolve up to 10-mol% CdS without crystallization. In comparison, GeS_2–Sb_2S_3 glasses can dissolve up to 20-mol% CdS, implying that Sb_2S_3 could delay the construction of [Cd_4GeS_6] polyhedron and increase the dissolving amount of CdS in the glass.

Keywords: chalcogenide glass, Raman spectroscopy, structure, Ge–Sb–Cd–S system

PACS: 42.70.Ce, 42.70.Km, 36.20.Ng **DOI:** 10.1088/1674-1056/26/10/104208

1. Introduction

Chalcogenide glasses, which are amorphous materials based on the chalcogen elements S, Se, and Te alloyed with group III–V elements such as Ga, Ge, As, and Sb, have received considerable attention for several decades. They have many important optical applications in the infrared (IR) such as lenses,[1,2] transmitting fibers,[3,4] sensors,[5–7] imaging bundles,[8,9] lasers & amplifiers,[10–12] nonlinear waveguides,[13–16] and diffraction gratings,[17] stemming principally from their unique properties of excellent IR transparency, low phonon energy, high linear and nonlinear refractive index, and large photosensitivity. A more attracting characteristic of chalcogenide glass is good solubility for metal sulfide or halide, which makes it convenient to adjust its physical properties for different uses.[18–20] For example, GeS_2–Sb_2S_3–CdS chalcogenide system has a large glass-forming region which is mainly situated along the GeS_2–Sb_2S_3 binary side, and the content of CdS in the glass could be as high as 30 mol%.[18] Depending on the composition, the glass has a glass transition temperature of 293 °C–310 °C, a linear refractive index of 1.95–2.43 (n_D), a density of 2.99 g·cm^{-3}–3.29 g·cm^{-3} and a micro-hardness of 158.9 kg·mm^{-2}–250.9 kg·mm^{-2}.[18] Besides, the glass has ultrafast ($\sim$ 100 fs) and high third-order optical nonlinearity ($\chi^{(3)} \approx 8.3 \times 10^{-13}$ esu),[21] and large electrical/thermal poling induced second-order nonlinear susceptibility ($\chi^{(2)} \approx$ 9 pm/V).[22]

It is known that macroscopic physical properties and microscopic connectivity of the glass network have a close relationship.[23,24] In order to tune the properties of chalcogenide glass in a relatively large range, the chalcogenide system is expect to be capable of dissolving a high concentration of modifiers (e.g., metal sulfides, halides, etc.). Hence, it is necessary to understand the flexibility of the chalcogenide glass structure and the contributions of constituent elements (or compounds). In this work, the network structures of pseudo-binary GeS_2–Sb_2S_3, GeS_2–CdS, Sb_2S_3–CdS, and pseudo-ternary GeS_2–Sb_2S_3–CdS chalcogenide systems are studied systematically by Raman spectroscopy. Their characteristic Raman bands are compared and analyzed. We aim to

*Project supported by the National Natural Science Foundation of China (Grant Nos. 61475189, 61405240, and 61575086), the Natural Science Basic Research Project in Shaanxi Province, China (Grant No. 2015JQ5141), and the Jiangsu Key Laboratory of Advanced Laser Materials and Devices, Jiangsu Normal University, China (Grant No. KLALMD-2015-08).

†Corresponding author. E-mail: guoht_001@opt.ac.cn

‡Corresponding author. E-mail: yangzhiyong@jsnu.edu.cn

© 2017 Chinese Physical Society and IOP Publishing Ltd

elucidate the contributions of the glass formers and modifiers to the network structure, and therefore provide guidance for tuning glass compositions for different uses.

2. Experimental procedures

The glass-forming region of GeS_2–Sb_2S_3–CdS pseudo-ternary system[18] and the compositions investigated in the present work are shown in Fig. 1. Two pseudo-binary and three pseudo-ternary glass groups were probed. In addition, $50Sb_2S_3$–50CdS crystalline sample was prepared using a similar preparation process for the structure investigations. The samples were prepared by the melt-quenching technique from high purity Ge, Sb, and S (5N in purity) and spectral-grade CdS (4N in purity). The preparation procedure was similar to that detailed in Ref. [19].

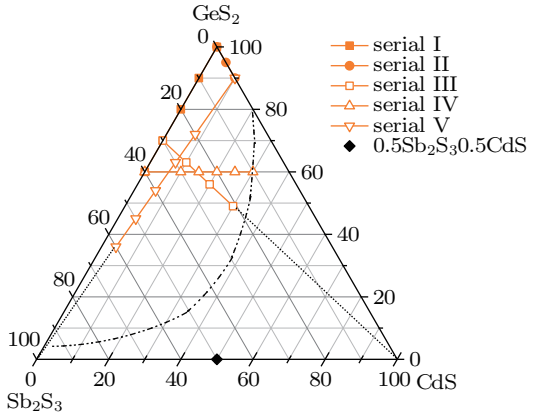


Fig. 1. (color online) Glass-forming region of GeS_2–Sb_2S_3–CdS pseudo-ternary system[18] and compositions investigated in this work. Series I: $(100-x)GeS_2 \cdot xSb_2S_3$; Series II: $(100-x)GeS_2 \cdot xCdS$; Series III: $(100-x)(0.7GeS_2 \cdot 0.3Sb_2S_3) \cdot xCdS$; Series IV: $60GeS_2 \cdot (40-x)Sb_2S_3 \cdot xCdS$; Series V: $(100-x)$ $(0.9GeS_2 \cdot 0.1CdS) \cdot xSb_2S_3$. The lines are drawn as guides for the eye.

The Raman spectra were measured at room temperature by a Raman Spectrometer (Renishaw RM-1000) in back (180°) scattering mode. An He–Ne laser (632.8 nm) was used as the excitation. To avoid laser damage to the sample and local crystallization of the glass, the laser power was properly under an approximate level of about 2 mW. The resolution of the Raman spectra was 1 cm^{-1}. Powder x-ray diffraction (XRD) patterns were recorded using a Rigaku D/max-RB diffractometer with Cu-Kα radiation. The operating voltage was 40 kV and the current was 50 mA.

3. Results and discussion

For each of the investigated glasses, no evident vibrational band in a region of 600 cm^{-1}–3000 cm^{-1} is found in the Raman spectra, and therefore only the data below 600 cm^{-1} are presented. Besides, the Raman bands below 150 cm^{-1} are complicated and difficult to accurately identify, hence they will not be discussed in the following text. Previous studies indicated that the Raman spectrum measured directly from the spectrometer could not reflect the pure structural changes and must be corrected to temperature and frequency factors. The corrected spectrum was defined as reduced Raman spectrum.[25,26] The reduced Raman intensity (I^{red}) is directly proportional to the intrinsic molar scattering factor and it can be obtained from the experimentally measured one (I^{exp}) by using the following equations:[25,26]

$$I^{red}(\omega) = (\omega_0 - \omega)^{-4}\omega[n(\omega,T)+1]^{-1}I^{exp}(\omega), \quad (1)$$

$$n(\omega,T) = [\exp(\hbar\omega/k_BT)-1]^{-1}, \quad (2)$$

where ω is the Raman shift in unit cm^{-1}, ω_0 is the wavenumber of the incident radiation, T is the absolute temperature, h is the Planck constant, and k_B is the Boltzmann constant. For distinguishing overlapped vibrational bands, the reduced Raman spectrum is deconvoluted into a series of Gaussian sub-bands[27] which are ascribed to specific vibrations of the structural units (SUs).

3.1. GeS_2–Sb_2S_3 pseudo-binary system

Figure 2 shows the Raman spectra of series I: $(100-x)GeS_2 \cdot xSb_2S_3$ ($x = 0$, 10, 20, 30, and 40) samples. Table 1 summarizes the assignments of the Raman shifts. After Sb_2S_3 is added into GeS_2 glass, three evident changes are observed: (i) the small band at 256 cm^{-1} disappears, and a broad band at around 170 cm^{-1}–200 cm^{-1} emerges; (ii) two new bands centered at 290 cm^{-1} and 314 cm^{-1} appear, and their intensities increase with increasing Sb_2S_3 content; (iii) the intensities of 340, 372, 400, and 430 cm^{-1} decrease with increasing Sb_2S_3 concentration.

Previous studies on the structure of vitreous GeS_2[42] indicate that in the GeS_2 glass, the basic SUs are corner-sharing and edge-sharing [GeS_4] tetrahedra which are connected through bridging sulfur atoms to form a three-dimensional network. The bands at 150, 340, 372, 400, and 430 cm^{-1} are associated with the vibrations of [GeS_4] tetrahedra and their assignments are listed in Table 1. It should be pointed out that the weak band at 150 cm^{-1} is usually difficult to accurately detect using normal Raman spectrometer, and therefore it is generally seldom considered in spectral analyses. Besides, the 290 cm^{-1} and 314 cm^{-1} bands are considered to be associated with the stretching vibrations of [SbS_3] pyramids with different connection styles (e.g., corner-sharing and edge-sharing pyramids).[31,34,35,43]

The measured Raman spectrum of GeS_2 (see Fig. 2, $x = 0$) shows that a small number of [S_3Ge–GeS_3] SUs (256 cm^{-1}) and -S-S-/S_8 ones (475 cm^{-1}) exist simultaneously in this stoichiometric composition. The former is because of the S deficiency whereas the latter is due to the S excess. This contradictory phenomenon could be caused by the local compositional fluctuations during the glass synthesis (influenced by melting temperature, time, quenching rate, etc.)[44,45] mainly because of the high viscosity of the GeS_2 melt. After Sb_2S_3 is added, stoichiometric Ge–Sb–S glass is formed. Compared with Sb, Ge is very likely to bond to S in

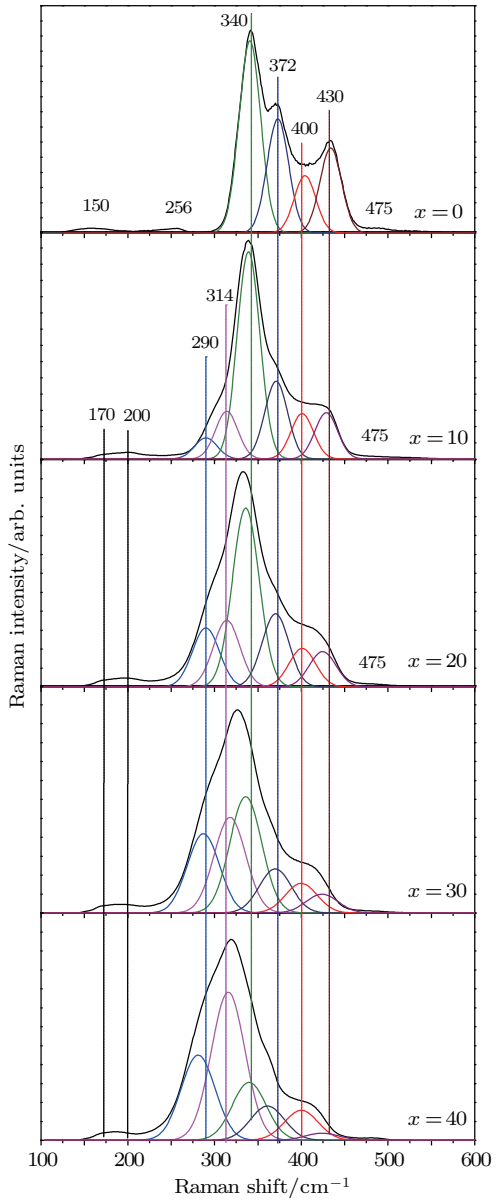


Fig. 2. (color online) Raman spectra of $(100-x)GeS_2 \cdot xSb_2S_3$ pseudo-binary samples.

Table 1. Raman shifts and assignments in GeS_2–Sb_2S_3 glasses.

Raman shift/cm^{-1}	Assignments	References
150	bending mode of [GeS_4]	[28], [29]
170	vibration of [S_2Sb–SbS_2]	[30], [31]
200	vibration of [S_2Sb=-GeS_3]	[32]
256	vibration of [S_3Ge–GeS_3]	[32], [33]
290	stretching mode of [SbS_3]	[31], [34]
314	stretching mode of [SbS_3]	[31], [34], [35]
340	symmetrical stretching mode of corner-sharing [GeS_4]	[31], [34], [36], [37]
372	stretching mode of edge-sharing [GeS_4]	[32], [38]
400	asymmetrical stretching mode of corner-sharing [GeS_4]	[28], [39]
430	stretching mode of edge-sharing [GeS_4]	[38], [40]
475	vibration of -S-S-bridging groups and/or of S_8 ring	[41]

the glass because of the higher bond energy of Ge–S than Sb–S.[46] This is similar to the situation in Ge–As–S–Se glass, where Ge has the priority to capture S over As.[47] For this reason, the local compositional fluctuation is more likely to lead to the formation of [S_2Sb–SbS_2] SU (170 cm^{-1}) instead of [S_3Ge–GeS_3] (256 cm^{-1}) ones, as shown in Fig. 2 ($x = 0$, $x = 10$). Simultaneously, some [S_2Sb–GeS_3] SUs (200 cm^{-1}) are also formed as indicated in Fig. 2 ($x = 10$–40). On the other hand, co-melting of Sb_2S_3 with GeS_2 reduces the viscosity of the melt and improves the homogeneity of glass, resulting in the decrease of -S-S-/S_8 groups in network. With the addition of Sb_2S_3, the [SbS_3] pyramid is formed in structure, and its concentration increases with increasing Sb_2S_3 amount as indicated in Fig. 2 ($x = 0$–40). Concurrently, the concentration of [GeS_4] tetrahedra deceases after Sb_2S_3 has been introduced into GeS_2 glass, leading to the intensity decrease of corresponding Raman bands as indicated in Fig. 2 ($x = 0$–40).

3.2. GeS_2–CdS pseudo-binary system

Figure 3 shows the Raman spectra of series II: $(100-x)GeS_2 \cdot xCdS$ ($x = 0$, 5, and 10) samples. The addition of CdS into GeS_2 glass former leads to two distinct changes in the Raman spectra. First, an additional weak band situated at 202 cm^{-1} emerges and its intensity increases with further addition of CdS. This band was not reported before. To identify the ascription of this band, the Raman spectrum of commercial crystalline CdS (99.99%, powders) is first measured (see Fig. 4). A band situated at 210 cm^{-1} is observed, expressing a little difference of location. Considering that the sample with 15-mol% CdS is crystalline and the crystalline phase is Cd_4GeS_6 according to the XRD pattern (see Fig. 5(a)), we synthesize the crystalline Cd_4GeS_6 by melting the mixed raw materials with a composition molar ratio of Cd : Ge : S = 4 : 1 : 6 and measure its Raman spectra (see Fig. 5(b)). It can be seen that the band situated at 202 cm^{-1} has a good accordance with a band relating to the vibration of crystalline Cd_4GeS_6. This implies that [Cd_4GeS_6] polyhedral could be formed in the $95GeS_2$·5CdS and $90GeS_2$·10CdS glasses. The appearance of [Cd_4GeS_6] polyhedra foretells a strong crystallization tendency of GeS_2–CdS system. The destructive effect of CdS on the original GeS_2 glass network is severe, and this explains why GeS_2 can dissolve only 10-mol% CdS,[18] while the glass can contain up to 90-mol% Sb_2S_3. The second change in the Raman spectra is the dissolution of the band at 256 cm^{-1} with the addition of CdS. It disappears due to the dissociation of metallic Ge–Ge bonds. Sulfur brought in with CdS can compensate for the sulfur deficiency resulting from the local compositional fluctuation and therefore convert [S_3Ge–GeS_3] SUs into [GeS_4] tetrahedra. On the other hand, CdS acts as a network modifier and tends to break some connections of [GeS_4] tetrahedra. In this case, non-bridging sulfurs (NBS)

are formed, and the Cd^{2+} ions act as charge compensators for them. It is worth mentioning that Raman spectra mainly detect network structure of the glasses, however, Cd^{2+} does not enter into the glass network, therefore the Raman spectra are not expected to show significant intensity changes of the bands associated with vibrations of [GeS_4] tetrahedra as indicated in Fig. 3. The weak band at around 475 cm^{-1} generally disappears, which indicates that co-melting of CdS with GeS_2 may also reduce the viscosity of the melt and improves the homogeneity of glass, resulting in the decrease of -S-S-/S_8 groups in network.

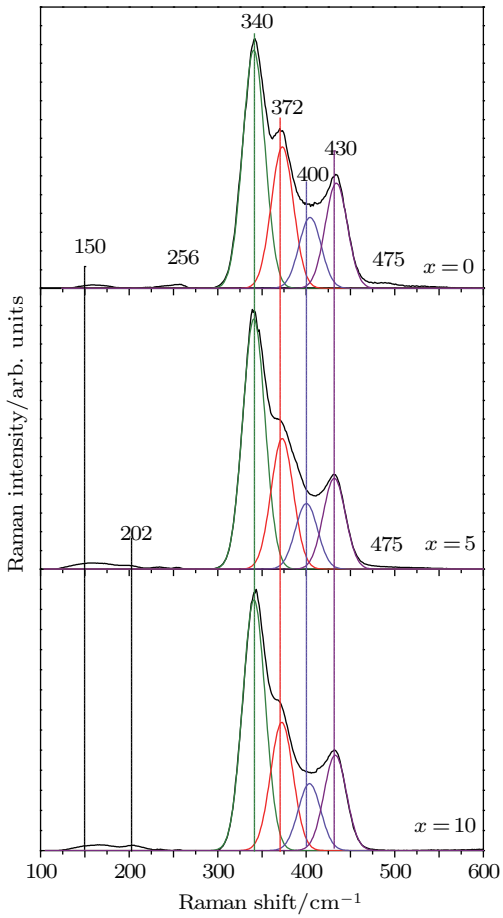


Fig. 3. (color online) Raman spectra of $(100-x)GeS_2 \cdot xCdS$pseudo-binary samples in the region of 100 cm^{-1}–600 cm^{-1}.

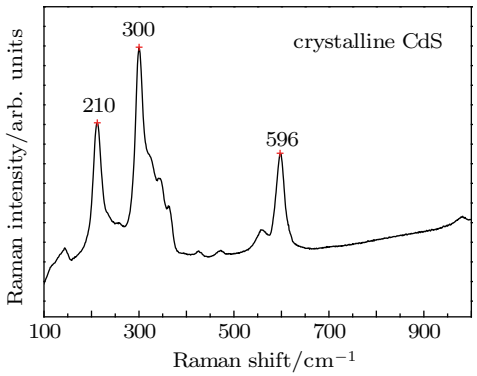


Fig. 4. (color online) Raman spectrum of crystalline CdS in the region of 100 cm^{-1}–1000 cm^{-1}.

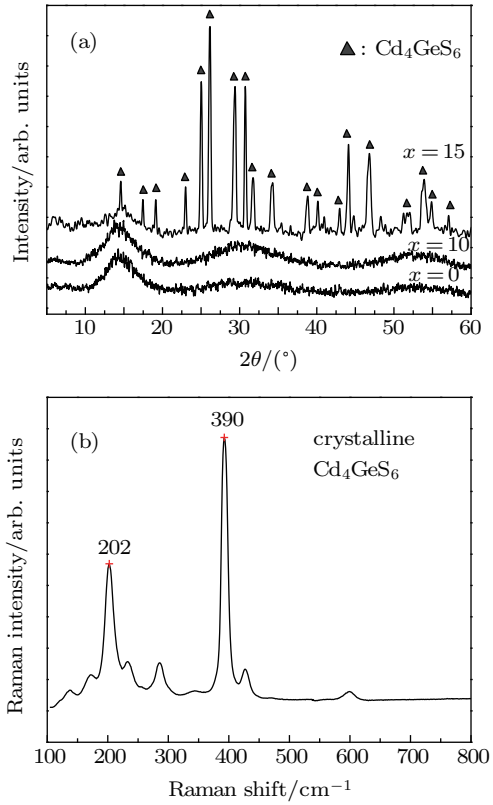


Fig. 5. (color online) (a) The XRD patterns of samples in $(100-x)GeS_2 \cdot xCdS$ pseudo-binary system; (b) Raman spectrum of crystalline Cd_4GeS_6.

3.3. Sb_2S_3–CdS pseudo-binary system

In order to judge whether new phase or SU could be formed in Sb_2S_3–CdS alloy, we synthesize the sample with $50Sb_2S_3 \cdot 50CdS$ composition using the same melt-quenching procedure described above. The sample is opaque, and shows a lead-gray color and metallic luster. Its XRD pattern is shown in Fig. 6. Only characteristic peaks of crystalline Sb_2S_3 and CdS are found, indicating that no new phase is formed.

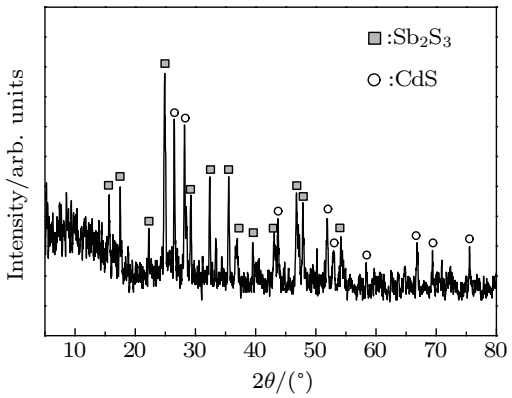


Fig. 6. XRD pattern of $50Sb_2S_3 \cdot 50CdS$ sample.

The Raman spectra of $50Sb_2S_3 \cdot 50CdS$ sample and crystalline Sb_2S_3 are presented in Fig. 7. Two similar but not identical spectra of $50Sb_2S_3 \cdot 50CdS$ sample are detected from different positions on the sample, showing its inhomogeneity and the occurrence of phase separation. Comparing them with

those of crystalline Sb_2S_3 and CdS, no new band is found, indicating the absence of new formed SU.

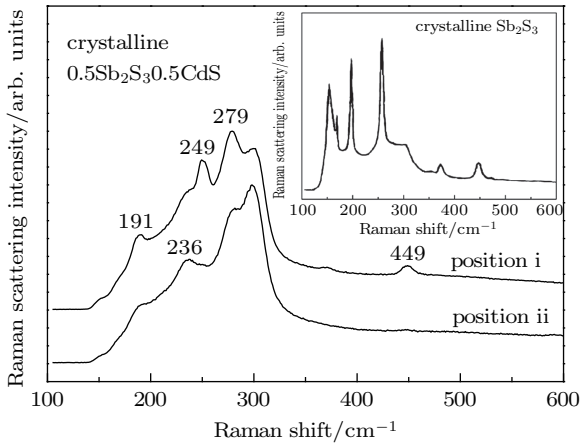


Fig. 7. Raman spectra of $50Sb_2S_3{\cdot}50CdS$ sample, with the insert showing the Raman spectrum of crystalline Sb_2S_3.

3.4. GeS_2–Sb_2S_3–CdS pseudo-ternary system

Figure 8 shows the Raman spectra of the series III: $(100-x)(0.7GeS_2{\cdot}0.3Sb_2S_3)\cdot x$CdS samples. With the addition of CdS into $0.7GeS_2{\cdot}0.3Sb_2S_3$ glass, two visible variations are observed: (i) the intensity of the 170-cm^{-1} band decreases ($x = 10$) and even disappears ($x \geq 20$), meanwhile, a new band at 202 cm^{-1} appears, and its intensity increases with increasing CdS concentration; (ii) the intensity of 290-cm^{-1} band increases, while that of 314-cm^{-1} band decreases, however the sum of the two intensities does not change significantly. To understand these variations, the role of CdS in the glass structure needs to be clarified. Additional sulfur comes with the addition of CdS. Considering that Cd^{2+} tends to acts as a charge compensator, there are sufficient sulfur atoms for Ge and Sb atoms to bond with. In this case, [S_2Sb–SbS_2] SUs do not form any more. Furthermore, Cd^{2+} does not enter into the glass network, thus the Raman spectra are not expected to show significant concentration changes of [GeS_4] and [SbS_3] network formers. Instead, the connection styles of the network formers may change due to the influence of CdS addition. This accounts for the intensity variations of the 290-cm^{-1} and 314-cm^{-1} bands.

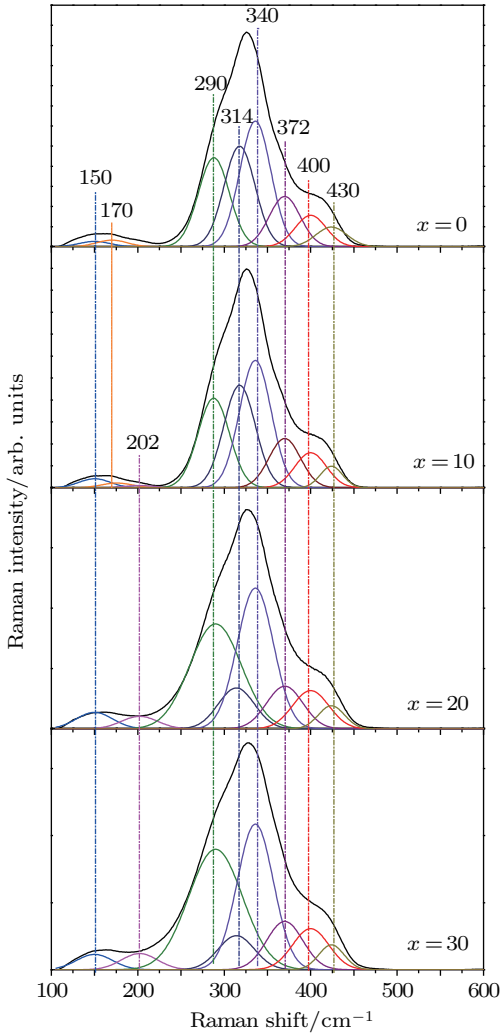


Fig. 8. (color online) Raman spectra of $(100-x)(0.7GeS_2{\cdot}0.3Sb_2S_3){\cdot}x$CdS pseudo-ternary system in the region of 100 cm^{-1}-600 cm^{-1}.

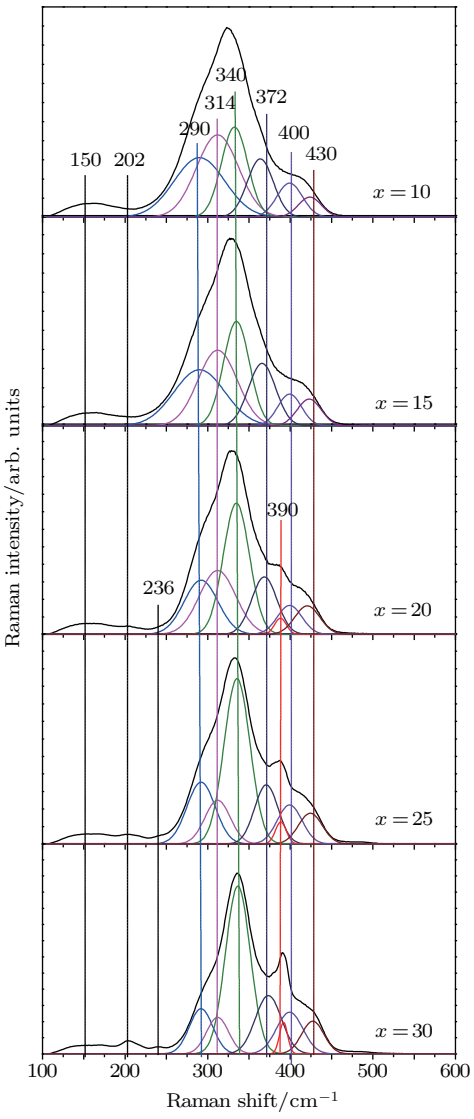


Fig. 9. (color online) Raman spectra of $60GeS_2{\cdot}(40-x)Sb_2S_3\cdot x$CdS pseudo-ternary system in the region of 100 cm^{-1}–600 cm^{-1}.

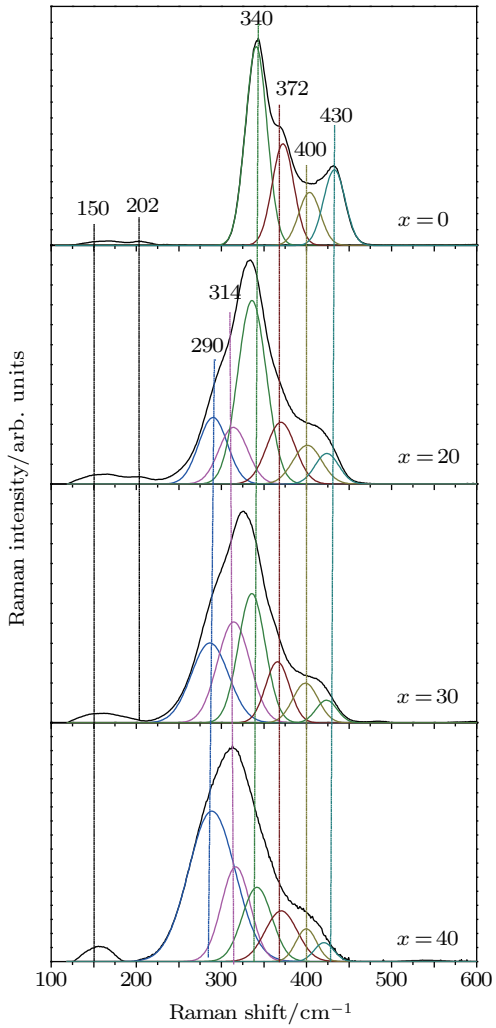


Fig. 10. (color online) Raman spectra of $(100-x)$ $(0.9GeS_2{\cdot}0.1CdS){\cdot}xSb_2S_3$ pseudo-ternary system in the region of 100 cm^{-1}–600 cm^{-1}.

Figure 9 shows the Raman spectra of the series IV: $60GeS_2{\cdot}(40-x)Sb_2S_3 \cdot xCdS$ samples. With increasing replacement of Sb_2S_3 by CdS, the intensities of 290-cm^{-1} and 314-cm^{-1} bands decrease because of the reduced number of $[SbS_3]$ pyramids in the structure. When more than 20-mol% Sb_2S_3 is substituted by CdS, three new bands at 202, 236, and 390 cm^{-1} emerge, and their intensities are enhanced with increasing CdS content. These three bands are all related to the vibrations of $[Cd_4GeS_6]$ polyhedra according to Fig. 5(b). When the CdS concentration is more than 20 mol%, the 202-cm^{-1} and 390-cm^{-1} bands become sharper, indicating the formation of crystalline Cd_4GeS_6. Compared with the GeS_2–CdS pseudo-binary system where $[Cd_4GeS_6]$ polyhedra are formed when CdS content is more than 10 mol%, the GeS_2–Sb_2S_3–CdS pseudo-ternary system does not contain $[Cd_4GeS_6]$ polyhedra until CdS concentration reaches 20 mol%. This indicates that the constituent Sb_2S_3 delays the construction of $[Cd_4GeS_6]$ polyhedron in the glass. Figure 10 shows the Raman spectra of the series V: $(100-x)$ $(0.9GeS_2{\cdot}0.1CdS){\cdot}xSb_2S_3$ glassy samples. It can be seen that the 202-cm^{-1} band disappears when more than 20-mol% Sb_2S_3 is added into $0.9GeS_2{\cdot}0.1CdS$ glass, proving again that Sb_2S_3 is able to delay the construction of $[Cd_4GeS_6]$ polyhedron.

4. Conclusions and perspectives

GeS_2 glass has a three-dimensional continuous network structure which consists of cross-linked corner-sharing and edge-sharing $[GeS_4]$ tetrahedra. A small number of ethane-like $[S_3Ge–GeS_3]$ SUs and -S-S-/S_8 groups also exist simultaneously in the structure probably due to local composition fluctuations. When Sb_2S_3 is added into GeS_2 glass, $[SbS_3]$ pyramids are formed. In addition, Ge atoms in $[S_3Ge–GeS_3]$ SUs are likely to capture S atoms from Sb_2S_3, leading to the formation of $[S_2Sb–SbS_2]$ SUs. The network backbone of the GeS_2–Sb_2S_3 glass consists of interconnected $[GeS_4]$ tetrahedra and $[SbS_3]$ pyramids. When CdS is introduced into GeS_2 glass, $[Cd_4GeS_6]$ polyhedra are formed. This glass can dissolve up to 10-mol% CdS without crystallization. Beside, Ge atoms in $[S_3Ge–GeS_3]$ SUs tend to capture S atoms from CdS, resulting in the dissolution of the SUs. Co-melting of Sb_2S_3 or CdS with GeS_2 can reduce the viscosity of the melt and improves the homogeneity of glass, leading to the disappearance of -S-S-/S_8 groups in local structure. When CdS is added into GeS_2–Sb_2S_3 glass, the network structure of the resulting glass does not change significantly. Compared with GeS_2 glass, GeS_2–Sb_2S_3 glass can dissolve up to 20-mol% CdS, suggesting that Sb_2S_3 could delay the construction of $[Cd_4GeS_6]$ polyhedron.

References

[1] Zhang X H, Guimond Y and Bellec Y 2003 *J. Non-Cryst. Solids* **326-327** 519
[2] Cha d H, Kim H J, Hwang Y, Jeong J C and Kim J H 2012 *Appl. Opt.* **51** 5649
[3] Yang Z Y, Gulbiten O, Lucas P, Luo T and Jiang S B 2011 *J. Am. Ceram. Soc.* **94** 1761
[4] Sanghera J and Gibson D 2014 *Chalcogenide glasses: Preparation, properties and applications* (Oxford: Woodhead Publishing), pp. 113–138
[5] Eggleton B J, Luther-Davies B and Richardson K 2011 *Nat. Photon.* **5** 141
[6] Lucas P, Coleman G, Jiang S B, Luo T and Yang Z Y 2015 *Opt. Mater.* **47** 530
[7] Ma P, Choi D Y, Yu Y, Yang Z Y, Vu K, Thach N, Mitchell A, Luther-Davies B and Madden S 2015 *Opt. Express* **23** 19969
[8] Zhan H, Yan X T, Guo H T, Xu Y T, He J L, Li F, Yang J F, Si J H, Zhou Z G and Lin A X 2015 *Opt. Mater.* **42** 491
[9] Zhang B, Zhai C C, Qi S S, Guo W, Yang Z Y, Yang A P, Gai X, Yu Y, Wang R P, Tang D Y, Tao G M and Luther-Davies B 2015 *Opt. Lett.* **40** 4384
[10] Guo H T, Liu L, Wang Y Q, Hou C Q, Li W N, Lu M, Zou K S and Peng B 2009 *Opt. Express* **17** 15350
[11] Seddon A B, Tang Z Q, Furniss D, Sujecki S and Benson T M 2010 *Opt. Express* **18** 26704
[12] Yang A P, Qiu J H, Zhang M J, Ren H, Zhai C C, Qi S S, Zhang B, Tang D Y and Yang Z Y 2017 *J. Alloys Compd.* **695** 1237
[13] Eggleton B J, Vo T D, Pant R, Schr J, Pelusi M D, Choi D Y, Madden S J, Luther-Davies B 2012 *Laser Photon. Rev.* **6** 97

[14] Petersen C R, Müller U, Kubat I, Zhou B, Dupont S, Ramsay J, Benson T, Sujecki S, Abdel-Moneim N, Tang Z, Furniss D, Seddon A and Bang O 2014 *Nat. Photon.* **8** 830

[15] Zhang B, Guo W, Yu Y, Zhai C C, Qi S S, Yang A P, Li L, Yang Z Y, Wang R P, Tang D Y, Tao G M and Luther-Davies B 2015 *J. Am. Ceram. Soc.* **98** 1389

[16] Ou H Y, Dai S X, Zhang P Q, Liu Z J, Wang X S, Chen F F, Xu H, Luo B H, Huang Y C and Wang R P 2016 *Opt. Lett.* **41** 3201

[17] Bernier M, El-Amraoui M, Couillard J F, Messaddeq Y and Vallée R 2012 *Opt. Lett.* **37** 3900

[18] Guo H T, Tao H Z, Gong Y Q and Zhao X J 2008 *J. Non-Cryst. Solids* **354** 1159

[19] Guo H T, Tao H Z, Gu S X, Zheng X L, Zhai Y B, Chu S S, Zhao X J, Wang S and Gong Q H 2007 *J. Solid State Chem.* **180** 240

[20] Yang Z Y, Tang G, Luo L and Chen W 2007 *J. Am. Ceram. Soc.* **90** 667

[21] Guo H T, Hou C Q, Gao F, Lin A X, Wang P F, Zhou Z G, Lu M, Wei W and Peng B 2010 *Opt. Express* **18** 23275

[22] Guo H T, Zheng X L, Lu M, Zou K S, Peng B, Gu S X, Liu H and Zhao X J 2009 *Opt. Mater.* **31** 865

[23] Xu H, Peng X F, Dai S X, Xu D, Zhang P Q, Xu Y S, Li X and Nie Q H 2016 *Acta Phys. Sin.* **65** 154207 (in Chinese)

[24] Yang Y, Chen Y X, Liu Y H, Rui Y, Cao F Y, Yang A P, Zu C K and Yang Z Y 2016 *Acta Phys. Sin.* **65** 127801 (in Chinese)

[25] Brooker M H, Nielsen O F and Praestgaard E 1988 *J, Raman Spectrosc.* **19** 71

[26] Andrikopoulos K S, Yannopoulos S N, Voyiatzis G A, Kolobov A V, Ribes M and Tominaga J 2006 *J. Phys: Condens. Matter* **18** 965

[27] Musgraves J D, Wachtel P, Gleason B and Richardson K 2014 *J. Non-Cryst. Solids* **386** 61

[28] Petit L, Carlie N, Adamietz F, Couzi M, V. Rodriguez and Richardson K C 2006 *Mater. Chem. Phys.* **97** 64

[29] Petit L, Carlie N, Villeneuve R, Massera J, Couzi M, Humeau A, Boudebs G and Richardson K 2006 *J. Non-Cryst. Solids* **352** 5413

[30] Kotsalas I P, Papadimitriou D, Raptis C, Vlcek M and Frumar M 1998 *J. Non-Cryst. Solids* **226** 85

[31] Zhang M J, Yang Z Y, Li L, Wang Y W, Qiu J H, Yang A P, Tao H Z and Tang D Y 2016 *J. Non-Cryst. Solids* **452** 114

[32] Nazabal V, Charpentier F, Adam J L, Nemec P, Lhermite H, Brandily-Anne M L, Charrier J, Guin J P and Moréac A 2011 *Int. J. Appl. Ceram. Tecnol.* **8** 990

[33] Guo H T, Zhai Y B, Tao H Z, Dong G P and Zhao X J 2007 *Mater. Sci. Eng. B-Adv.* **138** 235

[34] Yang A P, Zhang M J, Li L, Wang Y W, Zhang B, Yang Z Y and Tang D Y 2016 *J. Am. Ceram. Soc.* **99** 12

[35] Frumarová B, Nemec P, Frumar M and Oswald J 1998 *Semiconductors* **32** 812

[36] Heo J, Yoon J M and Ryou S Y 1998 *J. Non-Cryst. Solids* **238** 115

[37] Tao H Z, Mao S, Dong G P, Xiao H Y and Zhao X 2006 *Solid State Commun.* **137** 408

[38] Guo H T, Tao H Z, Zhai Y B, Mao S and Zhao X J 2007 *Spectrochim. Acta A* **67** 1351

[39] Hu J J, Tarasov V, Carlie N, Petit L, Agarwal A, Richardson K and Kimerling L 2008 *Opt. Mater.* **30** 1560

[40] Lin C G, Li Z B, Ying L, Xu Y S, Zhang P Q, Dai S X, Xu T F and Nie Q H 2012 *J. Phys. Chem. C* **116** 5862

[41] Kincl M and Tichy L 2007 *Mater. Chem. Phys.* **103** 78

[42] Feltz A, Pohle M, Steil H and Herms G 1985 *J. Non-Cryst. Solids* **69** 271

[43] Bayliss P and Nowacki W 1972 *Z. Kristallogr* **135** 308

[44] Julien C, Barnier S, Massot M, Chbani N, Cai X, Loireau-Lozac'h A M and Guittard M 1994 *Mater. Sci. Eng. B-Adv.* **22** 191

[45] Tverjanovich A, Tveryanovich Yu S and Loheider S 1996 *J. Non-Cryst. Solids* **208** 49

[46] Feltz A 1993 *Amorphous inorganic materials and glasses*, VCH, 100

[47] Sen S and Aitken B G 2002 *Phys. Rev. B* **66** 134204